

A FAULT FEEDER SELECTION METHOD FOR DISTRIBUTION NETWORK BASED ON EEMD

Shuxin Liu^{1*}, Yu Zhuo¹, Yanjun Zhang², Yundong Cao¹, Yuchen Cao³

1 School of Electrical Engineering, Shenyang University of Technology, China

2 Liaoning Electric Power Research Institute, China

3 Electrical Engineering of Tianjin University, China

ABSTRACT

In the case of small current grounding system, the fault current is too small to select the fault feeder. In order to solve this problem, this paper proposes a method based on Ensemble Empirical Mode Decomposition (EEMD) for fault feeder selection of distribution lines. Firstly, the zero-sequence current of all feeders is decomposed by the ensemble empirical mode decomposition, then the kurtosis calculation is performed on the decomposed Intrinsic Mode Function (IMF), and the transient high-frequency components are adaptively selected and the transient high-frequency energy is calculated. Defining fault credibility based on transient high frequency energy. Finally, the fault credibility of all feeders is compared, and the fault feeder selection result is given. The simulation results of PSCAD show that the method has high precision and is not affected by factors such as transition resistance, fault distance and initial fault angle.

Keywords: distribution network, small current grounding system, fault feeder selection, transient energy, eemd.

1. INTRODUCTION

Most of China's distribution network adopts the operation mode of small current grounding. This operation mode can make the system continue to run for a period of time after the fault occurs, but the fault current is not obvious, making fault feeder selection difficult. It is important to select the fault feeder to prevent further expansion and recovery of power supply.

The method of fault feeder selection is divided into transient method, steady state method and the combination of the two. After the fault occurs, it will

generate rich electrical transient information, so the current transient quantity based fault feeder selection method has received much attention. In [1], a single-phase ground fault selection method based on Prony algorithm is proposed. The fault feeder is determined by comparing the current of the dominant transient frequency of the fault feeder with the phase of the healthy feeder. In [2], wavelet transform is used to select the fault feeder according to the zero-sequence current transient reactive power direction, but the result of wavelet transform depends greatly on the choice of wavelet basis function. In [3], the zero-sequence current of the feeder is decomposed by Empirical Mode Decomposition (EMD) and the high-frequency transient energy maximum of the IMF is calculated to determine the faulty feeder. The EMD has the advantage of adaptability. However, modal aliasing occurs.

This paper proposes a fault feeder selection method based on EEMD, which preserves the advantages of adaptive decomposition of traditional EMD methods while overcoming the modal aliasing phenomenon that occurs in traditional EMD decomposition. The kurtosis is a fourth-order central moment that measures the degree of anomaly in the distribution. By comparing the maximum kurtosis of all IMFs, the most appropriate transient high-frequency component is selected. A fault credibility defined based on the transient high-frequency energy. By comparing the fault credibility, the fault feeder selection result can be accurately given. Through a large number of simulations and comparison with existing method, it is found that the fault feeder selection method proposed in this paper has good stability and is not affected by various fault factors.

2. ALGORITHM

2.1 EEMD algorithm

EMD can divide the signal into several IMF components and remainders by frequency. The essence of the EEMD algorithm is to use the uniformity of the Gaussian white noise frequency and its smoothing effect on the random interference component before performing EMD on the signal, adding random white noise to the original signal, and then iteratively analyzing the signal after the noise is added. Iteratively obtaining the IMF component can effectively solve the defect of modal aliasing generated by the EMD algorithm^[4]. The specific steps of the algorithm are as follows:

Step1: The original signal $x(t)$ is added to the random Gaussian white noise $N(t)$ with an amplitude coefficient of k to obtain $X(t)$:

$$X(t) = x(t) + kN(t) \quad (1)$$

Step2: EMD decomposition of $X(t)$ yields n IMF components and remainders:

$$X(t) = \sum_{h=1}^n c_h(t) + r_n(t) \quad (2)$$

Where $c(t)$ represents the IMF component obtained by the first EMD decomposition; $r(t)$ is the remainder obtained by the first EMD decomposition

Step3: Add different white noise $N_i(t)$ to $x(t)$, repeat steps 1 and 2 for m times, and obtain m group IMF components.

Step4: Calculate the mean of the IMF component of the m group as the result of the final EEMD decomposition. The calculation formula is:

$$c_i(t) = \frac{1}{m} \sum_{j=1}^m c_{jh}(t) \quad (3)$$

Where $c_i(t)$ represents the i th IMF component finally obtained.

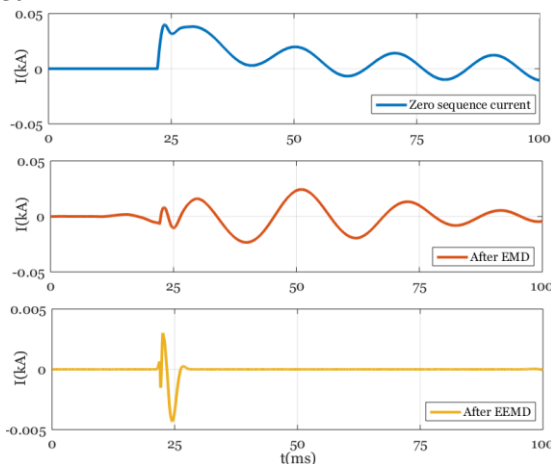


Fig.1 Comparison of zero-sequence current EMD and EEMD high-frequency components

The high-frequency components obtained by EMD and EEMD decomposition after the fault of the feeder are shown in Figure 1. The result of EMD decomposition has obvious modal aliasing, and the result of EEMD decomposition only contains transient high-frequency component.

2.2 Adaptive selection of IMF components

When the transition resistance is large, the transient high frequency component of the zero sequence current is not significant. As shown in Fig. 2, the first-order IMF obtained by EEMD is not a transient high-frequency component but a high-frequency noise, so the method of considering the first-order IMF component as a transient high-frequency component in the conventional method is not applicable.

The kurtosis can measure the abnormality of the signal distribution and is very sensitive to the transient mutation signal^[5]. The kurtosis K of the sample x is calculated as shown in equation (4):

$$K = \frac{E(x - \mu)^4}{\sigma^4} \quad (4)$$

Where μ is the average of x , σ is the standard deviation of x , and $E(x)$ is the expectation of sample x .

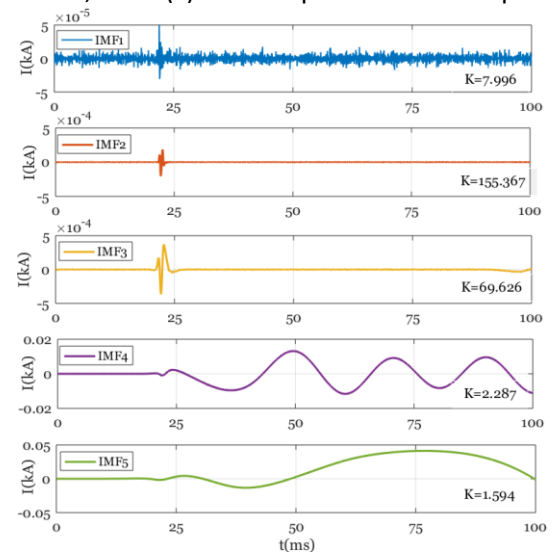


Fig.2 Various order IMF components obtained by EEMD decomposition

Table.1 Corresponding kurtosis of each order IMF component

| | IMF1 | IMF2 | IMF3 | IMF4 | IMF5 |
|---|-------|---------|--------|-------|-------|
| K | 6.966 | 155.367 | 69.629 | 2.287 | 1.594 |

For the IMF component decomposed by EEMD, the kurtosis is obtained separately, and the IMF with the largest kurtosis is the transient high-frequency com-

ponent. In the case of single-phase ground fault with large transition resistance, the IMF components obtained by EEMD decomposition are shown in Fig. 2. The kurtosis of each order of IMF components is shown in Table 1. By comparing the maximum kurtosis, we can find that the IMF2 component best matches the transient high-frequency component.

2.3 Fault feeder selection model

The fault feeder selection steps are as follows:

Step1: Extract the zero sequence current of all feeders after fault, perform EEMD operation according to Section 2.1, and adaptively select transient high-frequency IMF component according to Section 2.2.

Step2: The pre-judgment of the bus or feeder fault is achieved by the phase of the zero-sequence current high-frequency transient portion that is not affected by the arc-suppression coil:

$$|\vartheta_i - \vartheta_{\text{other}}| > 90^\circ \quad (5)$$

Where ϑ_i is the phase of the zero-sequence current at 2ms after the *i*th feeder fault occurs, and ϑ_{other} is the simultaneous phase of all the feeders except the *i*th feeder.

If the formula (5) is not established, the bus fault is judged; otherwise, the *i*-th feeder is pre-determined, and the step 3 is continued.

Step3: The high-frequency transient energy *E* is calculated as shown in equation (6).

$$E = \int_{t_0}^{t_0+T} C^2(t) dt \quad (6)$$

Where *C*(*t*) is the transient high-frequency component, *t*₀ is the fault start time, and *T* is the power frequency cycle.

Step4: Calculate the fault credibility of all feeders. The fault credibility *G* is calculated by the transient high frequency energy *E*.

$$G_i = \frac{E_i}{\sum_{j=1}^n E_j} \quad (7)$$

Where, *G_i* is the fault credibility of the *i*th feeder; *n* is the number of feeders in the distribution network.

Step5: Compare the value of the fault credibility of all feeders, and the feeder with the largest *G* value is judged as the fault feeder.

3. SIMULATION

A 10KV four-feeder distribution system is built in PSCAD. The topology is shown in Fig.3. The grounding method is resonant grounding, and the arc suppression coil compensation method is overcompensation, and the

compensation degree is 10%. All feeders are cables, and the parameters of the cables are shown in Table.2.

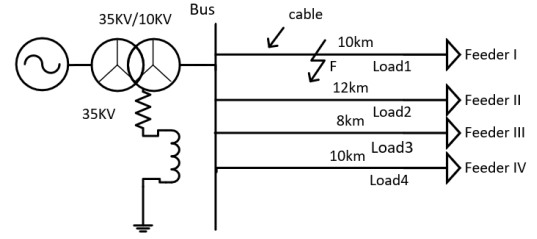


Fig.3 Simulation network topology

| | R(Ω/km) | L(mH/km) | C(uF/km) |
|-------------------|---------|----------|----------|
| Positive sequence | 0.2700 | 0.2228 | 0.3537 |
| Zero sequence | 2.7000 | 1.0164 | 0.3183 |

The zero sequence current of all feeders is obtained by simulation, and the transient high-frequency components are extracted and calculated by the method. For example, feeder 1 has a fault A phase ground fault at 40ms, the initial angle of fault is 0°, and the transition resistance is 100Ω. The zero sequence current of all feeders is shown in Fig.4, and the transient high-frequency component is extracted as shown in the Fig.5.

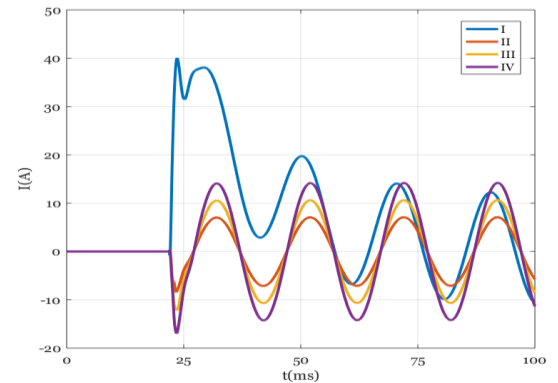


Fig.4 Zero sequence current of all feeders

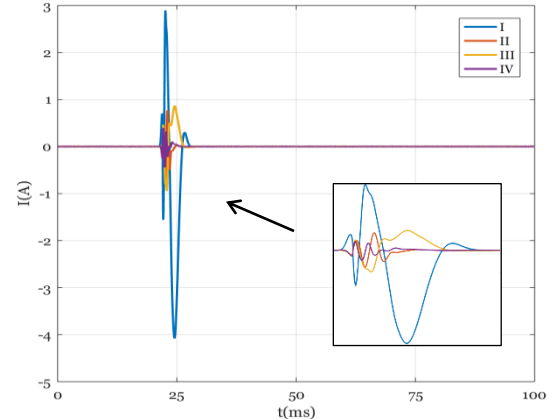


Fig.5 Comparison of transient high-frequency components of feeders

Fault distance D , fault initial angle ϑ , and transition resistance R_f were changed to perform a large number of simulations. The fault credibility of each feeder was calculated by the method proposed in this paper, and the fault feeder results were given. The results are shown in the Tables 3 to 5.

Table.3 Fault feeder results under different fault types(Phase A ground fault, $\vartheta = 0^\circ, R_f = 0\Omega$)

| Fault feeder | D | Fault credibility | | | Result | |
|--------------|------|-------------------|--------|--------|--------|---|
| I | 0km | 0.9896 | 0.0042 | 0.0023 | 0.0038 | I |
| I | 2km | 0.9907 | 0.0038 | 0.0019 | 0.0037 | I |
| I | 4km | 0.9961 | 0.0013 | 0.0009 | 0.0017 | I |
| I | 6km | 0.9890 | 0.0046 | 0.0025 | 0.0040 | I |
| I | 8km | 0.9916 | 0.0030 | 0.0022 | 0.0032 | I |
| I | 10km | 0.9894 | 0.0040 | 0.0026 | 0.0039 | I |

Table.4 Fault feeder results under different transition resistances(Phase A ground fault, $\vartheta = 0^\circ, D = 5\text{km}$)

| Fault feeder | R_f | Fault credibility | | | Result | |
|--------------|--------------|-------------------|---------------|---------------|--------|-----|
| I | 0Ω | 0.9896 | 0.0042 | 0.0023 | 0.0038 | I |
| I | 10Ω | 0.9767 | 0.0060 | 0.0075 | 0.0099 | I |
| II | 50Ω | 0.0094 | 0.9406 | 0.0233 | 0.0367 | II |
| II | 100Ω | 0.0050 | 0.9509 | 0.0236 | 0.0205 | II |
| III | 500Ω | 0.0067 | 0.0248 | 0.9377 | 0.0308 | III |
| III | 1000Ω | 0.0207 | 0.0361 | 0.8967 | 0.0466 | III |

Table.5 Fault feeder results under different initial angles of fault (Phase A ground fault, $R_f = 0\Omega, D = 5\text{km}$)

| Fault feeder | ϑ | Fault credibility | | | Result | |
|--------------|-------------|-------------------|---------------|---------------|--------|-----|
| I | 0° | 0.9896 | 0.0042 | 0.0023 | 0.0038 | I |
| I | 30° | 0.9910 | 0.0037 | 0.0021 | 0.0033 | I |
| II | 60° | 0.0030 | 0.9910 | 0.0017 | 0.0026 | II |
| II | 90° | 0.0010 | 0.9972 | 0.0006 | 0.0012 | II |
| III | 120° | 0.0009 | 0.0013 | 0.9961 | 0.0017 | III |
| III | 150° | 0.0016 | 0.0011 | 0.9954 | 0.0019 | III |

Under the same simulation conditions, the high-frequency transient energy extracted by EMD in the paper [3] and the feeder selection results under different transition resistances are shown in Table 6.

Table.6 Results of different method under different transition resistances(Phase A ground fault, $\vartheta = 0^\circ, D = 5\text{km}$)

| Fault feeder | R_f | Fault credibility | | | Result | |
|--------------|--------------|-------------------|---------------|---------------|--------|-----|
| I | 0Ω | 0.9845 | 0.0017 | 0.0034 | 0.1105 | I |
| I | 10Ω | 0.8517 | 0.0271 | 0.0841 | 0.0371 | I |
| II | 50Ω | 0.0594 | 0.8406 | 0.0533 | 0.0567 | II |
| II | 100Ω | 0.0550 | 0.8509 | 0.0736 | 0.0205 | II |
| III | 500Ω | 0.1488 | 0.1466 | 0.3844 | 0.3162 | III |
| III | 1000Ω | 0.2272 | 0.0810 | 0.3607 | 0.3311 | III |

Comparing the results of Table 3 to Table 5, it can be found that the feeder selection results in this paper are not affected by the fault distance, the transition resistance and the initial angle of the fault. Comparing Tables 4 and 6, it can be found that the method used in

the paper [3] has a small difference in the credibility between the faulty feeder and the non-faulty feeder when the transition resistance is large, which may cause misjudgment. The main reason is that the EMD will cause the model aliasing. The method proposed in this paper overcomes the modal aliasing and is better suited for faults with high transition resistance.

4. CONCLUSION

In view of the shortcomings of the existing methods, this paper proposes a complete fault feeder selection process. By simulating different fault conditions and comparing with existing methods, this method has the following advantages:

- The EEMD method preserves the advantages of traditional EMD adaptive decomposition while overcoming the modal aliasing defects of EMD.
- The kurtosis calculation is used to adaptively select the most suitable high-frequency transient component to avoid the erroneous selection caused by the fixed selection of the IMF component.
- Fault feeder and non-faulty feeders differ greatly in feeder selection results, and the method is not affected by various fault conditions.

The method proposed in this paper can solve the problem of fault feeder selection in the current resonant network grounding system, and has a good application prospect.

REFERENCE

- Zhang K, Zhang X, Xu B, et al. A novel single-phase earth fault detection method using DTF current phase[C]. International Conference on Electric Utility Deregulation & Restructuring & Power Technologies. IEEE, 2011.
- Wu X, Pan D, Zheng D. Research about single-phase fault feeder selection of small current neutral grounding system[C]. International Conference on Artificial Intelligence. IEEE, 2011.
- Liu Y. Research on Fault Detection and Fault Source Location Method of Distribution Network Cable Line[D].2015.
- Wu X, Yang M, Yuan X. Bearing fault diagnosis based on kurtosis criterion EEMD and improved morphological filtering method[J]. Journal of Vibration and Shock, 2015(2).
- Islam K A, Tcheslavski G V. Independent Component Analysis for EOG artifacts minimization of EEG signals using kurtosis as a threshold[C]. International Conference on Electrical Information & Communication Technology. IEEE, 2016.